Eur. Phys. J. D (2017) 71: 101
DOI: 10.1140/epjd/e2017-70570-7

THE EUROPEAN PHYSICAL JOURNAL D

Regular Article

Improving optical absorption in a-Si thin films with TiO_2 Mie scatterers

Giorgos Giannakoudakis[1] and Marcel Di Vece[1,2,3,a]

[1] Nanophotonics – Physics of Devices, Debye Institute for Nanomaterials Science, Utrecht University, P.O. Box 80000, 3508 TA Utrecht, The Netherlands
[2] Laboratory of Solid State Physics and Magnetism, Department of Physics and Astronomy, KU Leuven, Celestijnenlaan 200D, 3001 Leuven, Belgium
[3] CIMAINA and Dipartimento di Fisica, Università di Milano, via Celoria 16, 20133 Milano, Italy

Received 8 September 2016 / Received in final form 5 February 2017
Published online 25 April 2017

Abstract. To increase the optical absorption in very thin a-Si films is relevant for more efficient and inexpensive photovoltaics. In this work we deposited TiO_2 particles with a gas aggregation source on top of a-Si thin films and study the effect on optical absorption. When using thin films, anti-reflection and enhanced-reflection occurs depending on the thickness, which was employed in this study. The experiments were compared with finite difference time domain (FDTD) simulations which yielded good agreement. Both increased and decreased optical absorption was measured, depending on the photon energy range. This work demonstrates that by tailoring the various parameters, the TiO_2 particles can contribute to increasing the efficiency of an a-Si based solar cell.

1 Introduction

The investigations using novel concepts such as plasmonics and elongated nanostructures are gaining importance in thin film solar cell research [1] and photo catalysis [2].

One new approach to more efficiently couple light into a solar cell is the use of Mie scatterers for thin film solar cells as these are not suitable for standard light trapping techniques [3,4]. In a Mie scatterer, usually a dielectric particle such as silicon [5] for example, with the dimension of the wavelength of light (down to 10%), the scattering of light often has a stronger intensity in the forward direction which is useful when a light absorbing material is placed beneath it. The forward scattering enables the light to couple efficiently into the layers below it [6]. Since a Mie scatterer is made out of a dielectric material and not a metal with electric resistance acting on the plasmonic resonance, its optical losses are minimal [4]. When the Mie scatterer is large, the captured light will resonate at particular wavelengths, depending on the interference conditions, which enhances its optical cross section for these wavelengths. The circulating light in this Mie scatterer can be coupled into a solar cell beneath it by leaking, which makes a more efficient and selective harvesting of light possible. Mie scattering can provide a broad band optical absorption with for example silicon nanocone arrays [7]. The Mie scatterer is not limited to solar cells but can also be employed in solar fuel generation by light [8,9] The Mie scatterer composition can be chosen to obtain the desired optical properties as shown by using silicon carbide [10] silica [11] and germanium [12] particles.

In most of the current research of Mie scatterers for solar cells, top down techniques such as lithography and laser printing [13] is used to create the desired nanostructures. This is commercially not viable and therefore alternative methods (i.e. bottom up) to fabricate Mie scatterers for solar cells need to be explored. Although wet chemical techniques are used to fabricate Mie scattering structures [14,15], more industrial compatible techniques are desirable.

In this work we investigate the optical interaction of TiO_2 Mie scatterers with a-Si thin films. TiO_2 has been used as Mie scattering composite in dye sensitized solar cells [16] and has a sufficient high refractive index. Thin a-Si films are used in solar cells and can also function as a photovoltaic model system. Since TiO_2 is inexpensive, it could lead to a reduction of the amount of a-Si in the solar cell. TiO_2 has a high refractive index (2.6 [17]) and has been investigated before as a scatterer for solar cells [18]. Here the TiO_2 Mie scatterers are fabricated with a gas phase aggregation cluster source [19,20] which is fast, cheap, vacuum compatible and provides ultra-clean and well defined particles. Additionally, for thin film solar cells, conventional light management strategies don't work due to their large size [21], which is circumvented in this approach. Previously TiO_2 particles were produced by a pulsed microplasma cluster source [22], which demonstrates its versatility. Although the gas aggregation cluster

[a] e-mail: marcel.divece@unimi.it

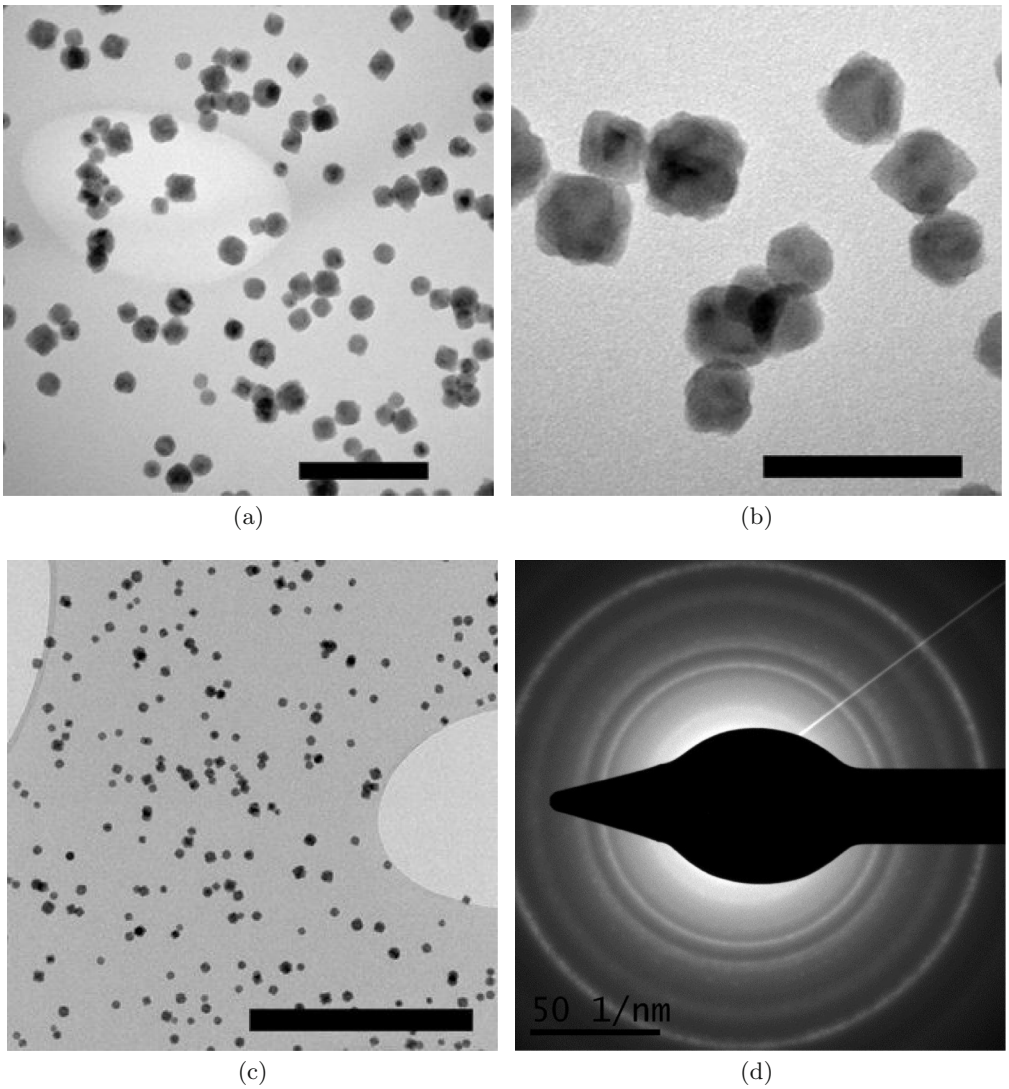

Fig. 1. (a, b) TEM images of TiO_2 particles produced by the gas phase aggregation cluster source. The shape of the particles is predominantly cubic. In (c) the uniformity of the deposition is clear. (d) An electron diffraction pattern in which the clear rings confirm crystallinity. The scale bars are for (a) 100 nm, (b) 40 nm and (c) 400 nm.

source has recently been used for photovoltaic investigations [23], the use of a cluster source for photovoltaics remains a very novel approach. After deposition of the TiO_2 particles on a-Si layers the systems were studied by measuring the optical transmission and reflection, from which the optical absorption could be determined.

Strong forward scattering of the TiO_2 particles, depending on the film thickness and composition, allow the detailed study of the optical cross section of such structures and the efficiency with which light is re-directed. This work opens a very promising new research avenue by using cluster sources for energy related research.

2 Experimental

The TiO_2 nanoparticles were produced by a gas aggregation magnetron sputtering cluster source (NC200U-B, Oxford Applied Research Ltd.) in DC mode with a power of 120 W and Ar flow of 10 to 20 sccm [24–26]. The TiO_2 target had a purity of 99.99%. The background and operation pressure were 2×10^{-8} and 1.7×10^{-3} mbar respectively with a total deposition time of up to 10 min per sample. The TiO_2 particle yield was 2.5 particles/μm^2/min.

The TiO_2 particles were also investigated by deposition on an a-C TEM grid after which transmission electron microscopy (TEM) was performed as shown in Figures 1a–1c. Although the cubic shapes are predominant, other shapes such as hexagonal, rhomboid, "cauliflower" [27] like particles, which are agglomerates of smaller particles are also present. Each TiO_2 deposition produces a different ratio of these particles shapes, leading to slightly different optical response. TEM electron diffraction analysis of the particles as shown in Figure 1d, provided lattice distances of 2.57 Å, 2.26 Å, 1.71 Å

en 1.48 Å which correspond well with a mixture of rutile and anatase structures. The samples selected for this work agreed best with the simulations and therefore likely consist mainly of cubic particles.

The a-Si thin films were obtained by magnetron sputtering (AJA International, Inc.) with 120 W and 40 sccm Ar flow of a Si target (99.9% purity). The background and operation pressure were 2×10^{-7} and 1×10^{-2} mbar respectively for the production of two nominally 30 and 70 nm thin films. The reasons for choosing 30 and 70 nm thick films was first of all to have the thickness as small as possible and still maintain reasonable optical absorption. The very thin a-Si film solar cell is commercially very interesting. Moreover, for this work it was necessary to not have maximum optical absorption in order to be able to measure optical absorption increases by the TiO2 particles. Another complication of much thicker a-Si films is the presence of multiple interference effects which were avoided by choosing such a thin film. The root mean square (RMS) roughness values of the 30 and 70 nm films were 1.6 and 1.8 nm respectively. This is extremely smooth and this thickness variation will not influence the results at all.

The total reflection, diffuse reflection and transmission were measured with an Agilent - Cary 5000 (Varian) spectrometer, which includes an integrating sphere. The wavelength range was selected from 250 nm to 1200 nm and as a reference a blank glass substrate was used. To obtain the optical response of the TiO_2 particles exclusively, the difference of a sample with and without TiO_2 particles was used.

Finite-difference time-domain (FDTD) simulations in 3D were performed with commercial software (Lumerical Solutions Inc.) on a flat a-Si layer (30 and 70 nm) with cubic TiO_2 particles of three different sizes: 20, 40 and 70 nm. To simulate a fully periodic and infinitely uniform distribution of TiO_2 particles we used Bloch boundary conditions in the direction of incident light, while in the perpendicular direction periodic (anti)-symmetric boundaries were used to reduce calculation time. The simulation area had a length and width of 513 and 560 nm. Below and above the layer with particles perfect matching layers (PML) were used to absorb the light. Advanced power absorption monitors were placed inside the structures. The pulse length of the incident plane wave was 50 fs with a band width of 8.825 THz. A convergence test was performed which confirmed sufficient accuracy with a smallest mesh size of 2 nm^3 on the TiO_2 particle.

The TiO_2 particles were deposited on a-Si thin films with two different thicknesses. This was necessary because the interference of light in and on a thin film causes two effects: (1) destructive interference in reflection, leading to strongly reduced reflection, which is used in products as anti-reflection coating, and (2) constructive interference in reflection, leading to a strong reflection (and reduced transmission). By selection of two a-Si thicknesses these two modes were explored in combination with TiO_2 Mie scatterers. The nominal thicknesses were 30 and 70 nm, which provides at 312 nm (3.97 eV) and 364 nm (3.41 eV) respectively. These resonant energies where chosen to overlap with the strong a-Si optical absorption in order to observe the maximal optical signal. The atomic force microscopy images of the TiO_2 particles on the a-Si thin films yielded clearly distinguishable particles with a densities of 53 and 54 particles/μm^2 for the 30 and 70 nm thin a-Si film respectively (Fig. 2).

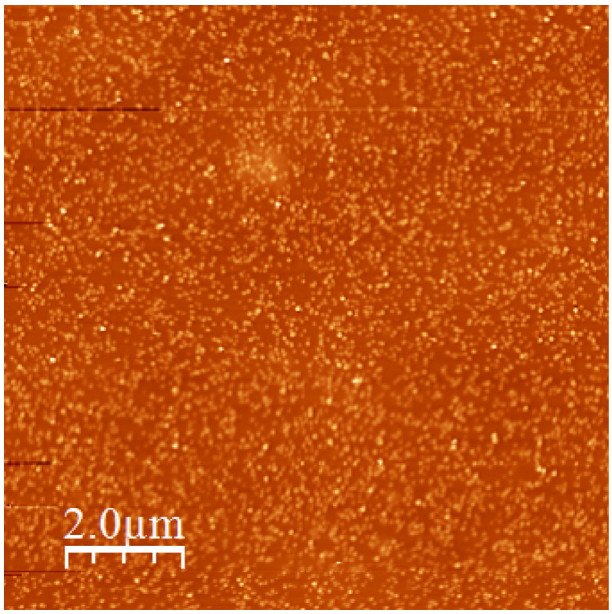

Fig. 2. Atomic force microscopy (AFM) micrograph of 70 nm a-Si film with TiO_2 nanoparticles on top.

3 Results

In Figure 3 the square TiO_2 nanoparticle on the a-Si thin film is schematically depicted for the condition of destructive (A) and constructive (B) interference for the reflected light. The light scattering of the TiO_2 particle is depicted as a dashed ellipse to indicate the large area of interaction. Since the scattering of light on a Mie particle results in a spectrally continuous (white) response [28], the scattered light therefore interferes with the incoming, reflected and transmitted light on the thin film.

In Figure 4a the optical absorptance of the 30 nm thick a-Si thin film with TiO_2 nanoparticles after subtraction with the reference a-Si film is shown. With this method the effect of only the TiO_2 particles on the optical response remains. A clear difference of several percent between the reference thin film and the thin film with TiO_2 particles is observed. The spectral shape of the absorptance difference is significantly different from the reference absorptance spectrum, indicating an independent effect of the TiO_2 particle.

The increase of absorptance difference going from the blue to the UV is caused by the optical absorption of TiO_2 with a band gap around 3.1 eV [29,30]. Since the solar spectrum (AM1.5) contains very little intensity at such energies, this effect is not relevant for photovoltaics. The absorptance increase of a few percent between 1 and 1.5 eV

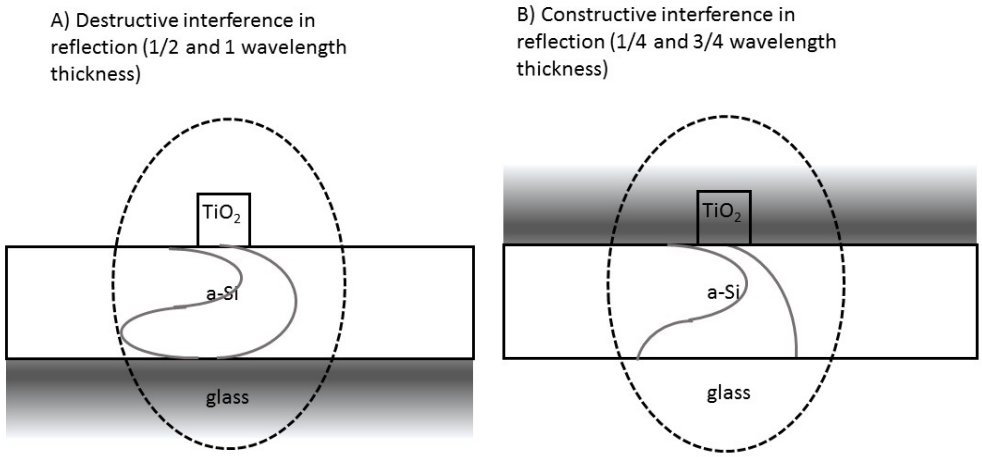

Fig. 3. The two possible optical properties of a thin a-Si film: (a) with destructive interference for reflection providing optimal absorption and transmission and (b) constructive interference for reflection, providing reduced absorption and transmission. The TiO_2 particle is expected to interact strongly with the strong field from reflection in situation (b).

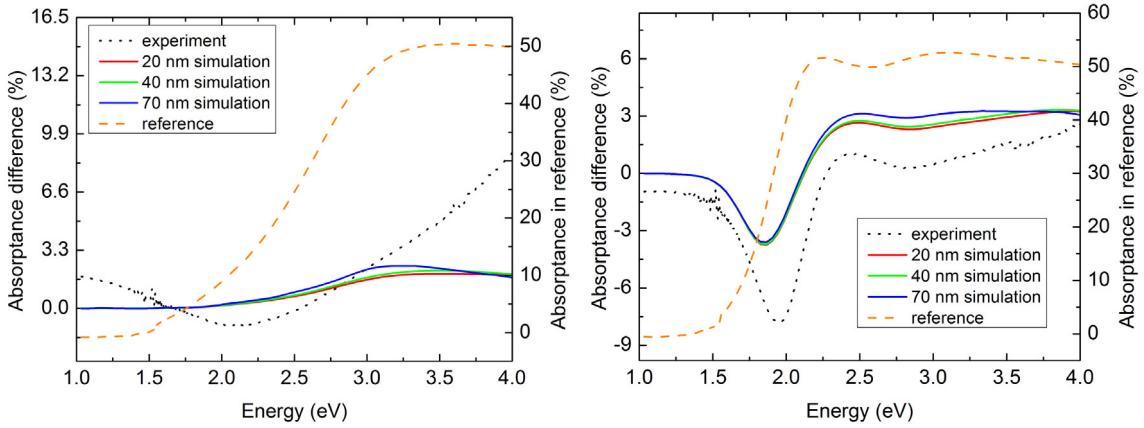

Fig. 4. Experimental (black) and simulated (red, green and blue) optical absorptance difference with a a-Si reference (orange) for (a) 30 nm (anti-reflection) and (b) 70 nm (anti-transmission) a-Si film. The different TiO_2 particle sizes are indicated by the colour. The reference a-Si thin film always has the same thickness as the a-SI thin film with TiO_2 particles.

and the reduced absorptance at about 2 eV is the result of light scattering on the TiO_2 particles. Considering the particle density of only 54 particles/μm^2 as obtained from AFM inspection, this is a strong response.

In the simulation of the different TiO_2 particle sizes, no significant absorptance difference is observed from 1 to 2 eV, possibly because the a-Si thin film does not absorbs light in that range. From about 2 eV until about 3 eV the absorptance difference increases in line with the experiment due to scattering. In contrast to the experiment the absorptance difference remains constant from 3 eV till the UV. The absence of a slope for the absorptance difference from 3 eV to the UV for the simulations is likely the result of the presence of defects in the experimental TiO_2 particles, which are optically very active. The difference in magnitude of the absorptance difference between experiment and simulation is the result of different TiO_2 particle surface density on the a-Si layer.

In Figure 4b the absorptance (difference) spectra for the 70 nm thin a-Si film with and without TiO_2 particles are shown. Except for a dip to negative values around 1.9 eV both the shape of the experimental and simulated graphs are very similar to the reference a-Si absorptance curve. The positive values of the absorptance difference over a wide spectral range suggests that the main effect of the TiO_2 particles is to increase the overall absorptance due to scattering. Since the 70 nm thin a-Si film has enhanced reflection, it may be argued that the scattering on the TiO_2 particles reduces the reflection, which leads to increased optical absorption.

The dip of the absorptance difference in both the simulation and experiment around 1.9 eV is the result of the reducing refractive index of a-Si. When the refractive index of a-Si is lower with respect to the refractive index of TiO_2, the scattering properties of the TiO_2 particles change and more light is scattered backward, away

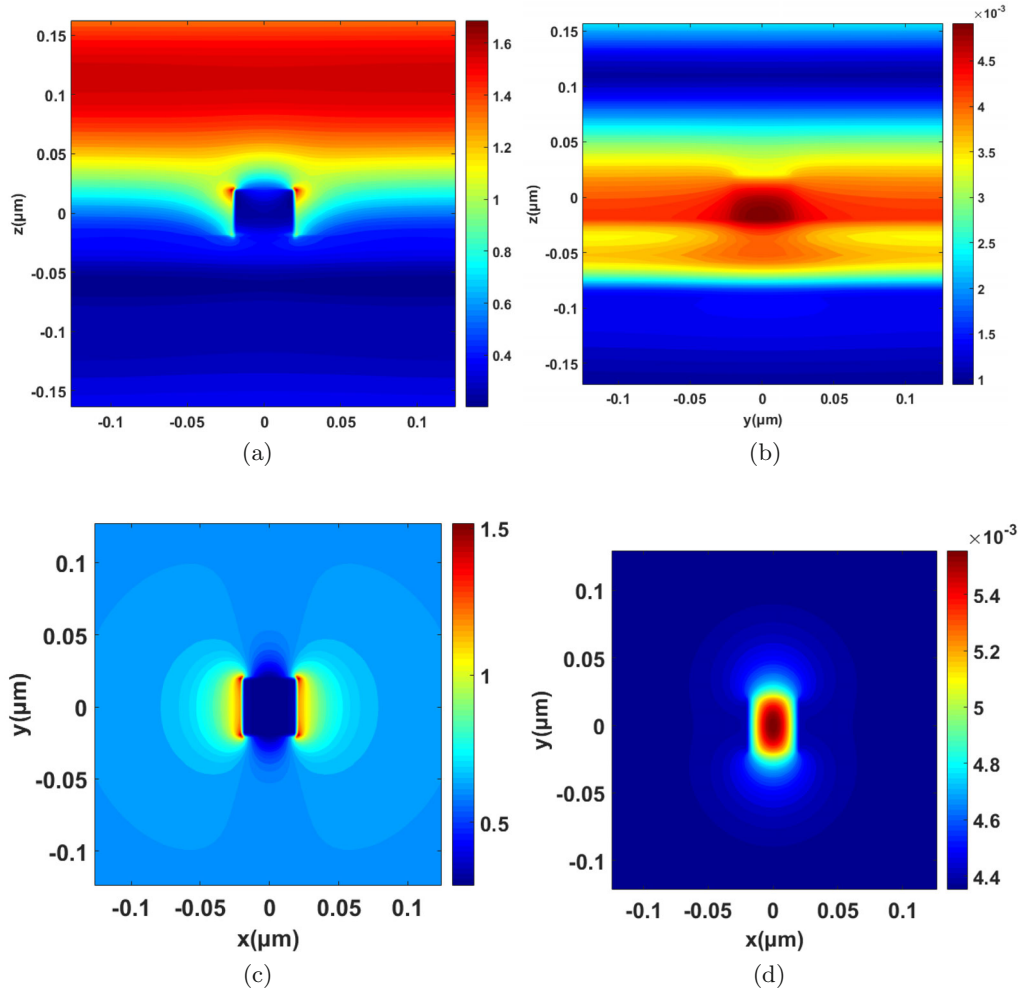

Fig. 5. Time integrated (a) E-field (logarithmic scale) and (b) H-field at 541 nm (2.29 eV) of 40 nm TiO_2 particle on 70 nm thick a-Si film (bottom part of graph). The high E-field intensity above the a-Si thin film confirms it anti-transmission properties. The TiO_2 particle affects both the E and H fields strongly at a local level. The E (logarithmic scale) and H field at the surface of the a-Si film underneath the 40 nm TiO_2 particle are shown in (c) and (d) respectively (450 nm).

from the a-Si thin film. The increasing absorptance from about 3.1 eV is again the result of optical absorption in defect rich TiO_2.

The results of the FDTD simulation for three particles of different size (20, 40, 70 nm) agree remarkably well with the experimental curves. The three different particle sizes show no discernible difference, which confirms that its Mie scattering properties, which are mainly size independent, dominate the optical effects. It is precisely this size independence of the Mie scattering of the TiO_2 particles, which enables such a good agreement between experiment and simulations.

The absorptance of the 30 and 70 nm thick films is similar around 50% because the increased reflection in the 70 nm film reduces its optical absorption and the reduced reflection of the 30 nm film increases its optical absorption.

In Figure 5 the E and H fields are shown in cross sections of the 40 nm TiO_2 particle on the 30 and 70 nm a-Si thin films. The choice of size and thickness is arbitrary since the different particle sizes and both a-Si thin films provide very similar results. From the pattern around the particles it is clear that the TiO_2 particles affect the electromagnetic field around it. The E-field is clearly distorted mainly outside the particle as can be seen from Figures 3a and 3c. It is known that the E-field induces displacement currents on the dielectric surface of a particle which result in a much stronger magnetic response [31] as can be seen from the high intensity H field inside the particle (Figs. 3b and 3d). These cross sections demonstrate the significant electromagnetic interaction of the TiO_2 particles with the light field on an a-Si thin film.

Although the optical effects in both the experiment and simulation are in the order of a few percent, increasing the particle density on the a-Si thin film surface would significantly increase the optical interaction and subsequently optical absorption. Since this is only a proof of principle study, future research towards device should explore the various parameters in more detail.

4 Conclusion

The presence of optical broad band Mie scattering of TiO_2 particles in the fields of constructive or destructive interference on a thin a-Si film results in a complex interaction. For the thin anti reflecting and enhanced reflection a-Si films, both increased and decreased optical absorption has been observed for certain photon energy ranges. The TiO_2 particles absorb photons larger than the band gap of TiO_2 which was particularly strong in the experiment due to defects. The experiment and simulations agreed well on many spectral features in the different systems. This study of TiO_2 Mie scatterers on an a-Si thin films contributes to making very thin a-Si films more efficient light absorbers, which may contribute to a photovoltaic device based on this effect.

The authors thank Hans Meeldijk, Marijn van Huis, and Da Wang for TEM and electron diffraction measurements. This work has been supported by a Marie Curie Career Integration Grant, Project No. 293687.

Author contribution statement

Marcel Di Vece conceived, and supervised the work. Giorgos Giannakoudakis performed the experiments and simulations. Di Vece and Giannakoudakis both wrote the manuscript.

References

1. H. Atwater, A. Polman. Nat. Mater. **9**, 205 (2009)
2. M. Di Vece, A.B. Laursen, L. Bech, C.N. Maden, M. Duchamp, R.V. Mateiu, S. Dahl, I. Chorkendorff, J. Photochem. Photobio. A: Chem. **230**, 10 (2012)
3. M.L. Brongersma, Y. Cui, S. Fan, Nat. Mater. **13**, 451 (2014)
4. A.I. Kuznetsov, A.E. Miroshnichenko, M.L. Brongersma, Y.S. Kivshar, B. Luk'yanchuk, Science **354**, 6314 (2016)
5. P. Spinelli, A. Polman, IEEE J. Photovolt. **4**, 554 (2014)
6. P. Spinelli M.A. Verschuuren, A. Polman. Nat. Commun. **3**, 692 (2012)
7. Z.Y. Wang, R.J. Zhang, S.Y. Wang, M. Lu, X. Chen, Y.X. Zheng, L.Y. Chen, Z. Ye, C.Z. Wang, K.M. Ho, Sci. Rep. **5**, 7810 (2015)
8. S.J. Kim, I. Thomann, J. Park, J-H. Kang, A.P. Vasudev, M.L. Brongersma, Nano Lett. **14**, 1446 (2014)
9. H. Xu, X. Chen, S. Ouyang, T. Kako, J. Ye, J. Phys. Chem. C **116**, 3833 (2012)
10. J.A. Schuller, R. Zia, T. Taubner, M.L. Brongersma, Phys. Rev. Lett. **99**, 107401 (2007)
11. S. Nunomura, A. Minowa, H. Sai, M. Kondo, Appl. Phys. Lett. **97**, 063507 (2010)
12. L. Cao, J.-S. Park, P. Fan, B. Clemens, M.L. Brongersma, Nano Lett. **10**, 1229 (2010)
13. U. Zywietz, A.B. Evlyukhin, C. Reinhardt, B.N. Chichkov, Nat. Commun. **5**, 3402 (2014)
14. M. Karg, T.A.F. König, M. Retsch, C. Stelling, P.M. Reichstein, T. Honold, M. Thelakkat, A. Fery, Mater. Today **18**, 185 (2015)
15. M.J. Mendes, S. Morawiec, T. Mateus, A. Lyubchyk, H. Águas, I. Ferreira, E. Fortunato, R. Martins, F. Priolo, I. Crupi, Nanotechnology **26**, 135202 (2015)
16. S. Son, S.H. Hwang, C. Kim, J.Y. Yun, J. Jang, ACS Appl. Mater. Interfaces **5**, 4815 (2013)
17. J.R. Devore, J. Opt. Soc. Am. **41**, 416 (1951)
18. S.H. Kang, J.-Y. Kim, H.S. Kim, H.-D. Koh, J.-S. Lee, Y.-E. Sung, J. Photochem. Photobio. A: Chem. **200**, 294 (2008)
19. E. Barborini, I.N. Kholmanov, A.M. Conti, P. Piseri, S. Vinati, P. Milani, C. Ducati, Eur. Phys. J. D **24**, 277 (2003)
20. O. Polonskyi, T. Peter, A.M. Ahadi, A. Hinz, T. Strunskus, V. Zaporojtchenko, H. Biederman, F. Faupel, Appl. Phys. Lett. **103**, 033118 (2013)
21. S. Chattopadhyay, Y.F. Huang, Y.J. Jen, A. Ganguly, K.H. Chen, L.C. Chen, Mater. Sci. Eng. R **69**, 1 (2010)
22. E. Barborini, I.N. Kholmanov, P. Piseri, C. Ducati, C.E. Bottani, P. Milani, Appl. Phys. Lett. **81**, 3052 (2002)
23. T. van der Vliet, M. Di Vece, Thin Solid Films **603**, 404 (2016)
24. H. Haberland, M. Mail, M. Mossier, Y. Qiang, T. Reiners, Y. Thurner, J. Vac. Sci. Technol. A **12**, 2925 (1994)
25. W.A. de Heer, Rev. Mod. Phys. **65**, 611 (1993)
26. K. Wegner, P. Piseri, H.V. Tafreshi, P. Milani, J. Phys. D: Appl. Phys. **39**, R439 (2006)
27. W. Tang, J.J. Eilers, M.A. van Huis, D. Wang, R.E.I. Schropp, M. Di Vece, J. Phys. Chem. C **119**, 11042 (2015)
28. U. Kreibig, M. Vollmer, *Optical Properties of Metal Clusters* (Springer, Berlin, 1995)
29. K.M. Reddy, S.V. Manorama, A.R. Reddy, Mater. Chem. Phys. **78**, 239 (2002)
30. X. Chen, S.S. Mao, Chem. Rev. **107**, 2891 (2007)
31. J. van de Groep, A. Polman, Opt. Express **21**, 26285 (2013)